

## Designing Optimum Salinity and Injection Rates for Low Salinity Water Alternating Hydrocarbon Gas Injection at “B” Structure in “S” Field

Ariel Delano Massie<sup>1</sup>, Asep Kurnia Permadi<sup>1</sup>, Rochvi Agus Dewantoro<sup>2</sup>, Egi Adrian Pratama<sup>3</sup>, Muhammad Arif Naufaliansyah<sup>1</sup>

<sup>1</sup>Institut Teknologi Bandung, <sup>2</sup>Bass Oil Sukananti Limited, <sup>3</sup>Curtin University

### Abstract

The inability of primary and secondary recovery methods in maximizing oil recovery from existing fields and the lack of new major reserve discoveries have been the two main issues in the oil and gas industry these days. The best solution to solve both problems is by performing enhanced oil recovery (EOR). One of the recent EOR methods that have been developed by many researchers is low salinity water alternating gas (LSWAG) injection. In the LSWAG injection, the type of injection gas that is preferred to be used is hydrocarbon gas. However, there are still limited studies that discuss the implementation of low salinity water alternating hydrocarbon gas injection in prospective fields along with its possible mechanisms.

This study is conducted to design the low salinity water alternating hydrocarbon gas injection at a sandstone reservoir named "B" Structure in "S" Field, Indonesia. Injected water salinity, water injection rate, and gas injection rate are the parameters that become the focus of this study. Sensitivity study through reservoir simulation using a compositional simulator, CMG GEM<sup>TM</sup>, is performed to study the impact of these parameters on oil recovery by evaluating reservoir dynamic properties and to determine the optimum scenario.

The results of this study conclude that oil recovery increases as the injected water salinity decreases due to wettability alteration towards more water wet. On the other hand, oil recovery increases as the water injection rate and gas injection rate increase due to sweep efficiency improvement. The optimum design of the LSWAG injection, after considering the capacities of field facilities, yields a significant increase of recovery factor from base case. Moreover, this advanced method can reduce cost and gas emission as it utilizes the produced gas.

Keywords: low salinity water alternating hydrocarbon gas injection, salinity, injection rate, recovery factor

### Introduction

Enhanced oil recovery (EOR) has been a popular topic in the oil and gas industry these days due to its advantage in extracting more hydrocarbons after primary and secondary recovery. The lack of new major discoveries has forced the oil and gas companies worldwide to maximize the full potential of their existing fields through EOR. One of the EOR methods that have become the center of attention for many researchers is low salinity water injection (LSWI). LSWI is a waterflooding technique in which the salinity of the injected water is made lower than the initial formation water to improve oil recovery. This emerging EOR method could increase the oil recovery of a reservoir up to 20% of original oil-in-place (OOIP) compared to conventional waterflooding (Dang et al., 2015). The benefits of this method in terms of oil recovery have been proved by extensive laboratory experiments and pilot tests. The underlying mechanism of this method is still open for discussion but most of the proposed mechanisms to date

indicate that wettability alteration occurs in LSWI and improves the oil recovery.

One of the underlying mechanisms of LSWI that has been widely accepted and used by many researchers is multicomponent ionic exchange (MIE). According to Lager et al. (2008), multivalent cations on the reservoir rock surface bond to polar compounds in the oil phase (resin and asphaltene) forming organo-metallic complexes. At the same time, some organic polar compounds are adsorbed directly to the rock surface displacing the most labile cations. When the low salinity water is injected, MIE takes place, removing the organic polar compounds and organo-metallic complexes from the surface and replacing them with uncomplexed cations (Figure 1). The desorption of the compounds from clay surface leads to a more water-wet surface increasing oil recovery.

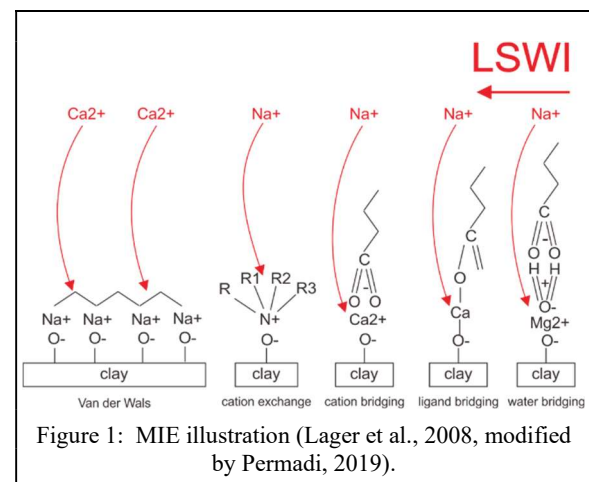


Figure 1: MIE illustration (Lager et al., 2008, modified by Permadi, 2019).

Recent studies on LSWI have discovered another significant benefit from the method when it is combined with another EOR method. One of the promising combinations is LSWI and gas injection, which is called low salinity water alternating gas (LSWAG) injection. LSWAG injection could promote the synergy of the mechanisms underlying LSWI and the mechanisms underlying gas injection (Dang et al., 2014). While LSWI encourages wettability alteration, gas injection enhances sweep efficiency through mobility ratio reduction and un-swept zone sweeping.

Based on its miscibility to the oil phase, gas injection can be classified into miscible and immiscible injection. The following explanation captures the mechanisms for immiscible injection only since the gas flooding process in this study is known to be immiscible. The two main mechanisms are oil swelling and viscosity reduction.

- a. Oil swelling  
Oil swelling increases the hydrocarbon saturation in a pore. When the saturation increases, the oil relative permeability and oil mobility in that pore increases as well. It leads

## PROCEEDINGS

JOINT CONVENTION BANDUNG (JCB) 2021

November 23<sup>rd</sup> – 25<sup>th</sup> 2021

- to a higher displacement efficiency and eventually higher oil recovery (Holtz, 2016).
- b. Viscosity reduction  
Viscosity reduction due to immiscible gas injection has been reported in various types of oil reservoirs including undersaturated, saturated, and heavy oils. Ning and McGuire (2004) found that oil viscosity reduction is found to be the dominant mechanism in severely undersaturated reservoirs. They explained that undersaturated oil can dissolve more gas than its initial GOR. When gas is injected into the reservoir, GOR increases, and oil viscosity decreases. Same as oil swelling, viscosity reduction also improves oil mobility.

For one cycle of injection, LSWAG injection consists of two steps, which are injecting low salinity water and injecting gas to the reservoir. The combination of viscosity reduction and oil swelling mechanisms from the gas flooding process has a significant impact on the mobility ratio and thus sweep efficiency of the low salinity waterflooding process (Holtz, 2016). It can be seen from the mobility ratio formula presented below.

$$M = \frac{k_{rw}\mu_o}{\mu_w k_{ro}}$$

Sweep mechanism is more stable when the mobility ratio value is less than 1. As explained before, oil swelling increases  $k_{ro}$  and decreases  $k_{rw}$ , while the viscosity reduction decreases  $\mu_o$ . All of which drive the mobility ratio towards a decreased value.

The most common injection gases used in the water alternating gas injection are CO<sub>2</sub> and hydrocarbon gas. Compared with CO<sub>2</sub>, hydrocarbon gas is preferable because it is usually directly available from production. In addition, rather than being flared, it is much more environmentally friendly when the produced gas is injected back to the reservoir. On the other hand, CO<sub>2</sub> is an expensive gas and not easily obtained. Moreover, corrosion problems are often reported when using CO<sub>2</sub> (Christensen et al., 2001; Dong et al., 2019). For those reasons, by using hydrocarbon gas as the injectant in its gas flooding process, LSWAG injection can be more attractive to be implemented in the oil fields.

This study is conducted to achieve several objectives that are limited to the application of low salinity water alternating hydrocarbon gas injection at a sandstone reservoir called "B" Structure in "S" Field. The objectives are presented below.

- a. To study the impact of injected water salinity, water injection rate, and gas injection rate on oil recovery.
- b. To determine the optimum design of injected water salinity, water injection rate, and gas injection rate which gives the highest recovery factor.

### Data and Method

"S" Field is an oil field located in South Sumatera Province, Indonesia. The field was found in 1990 with an area of approximately 4,510 acres. The field has two producing structures which are "B" and "T" Structure. This study

focuses only on the "B" Structure. This structure consists of three zones (sand layers): "T", "G", and "K" Sand Layers. "T" Sand Layers is the biggest and the main producing layer with 7.364 MMSTB of oil in place. Compared to the "T" Sand Layer, the two other sand layers are relatively small so that they are not included in this simulation study. Therefore, the "B" Structure in this paper only refers to the "T" Sand Layer. 2D Map of the "B" Structure is shown in Figure 2. There are three production wells (B-1, B-3, and B-5) currently producing from the "B" Structure and one suspended well (B-4). The three production wells had been producing 2.254 MMSTB of oil cumulative in total by December 2020.

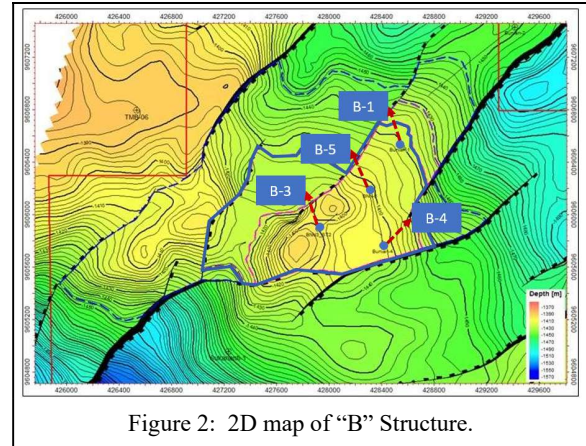


Figure 2: 2D map of "B" Structure.

The reservoir of the "B" Structure is a sandstone reservoir and belongs to Talang Akar Formation. It is reported to initially have 1,700 psig of reservoir pressure and 227 °F of reservoir temperature. The reservoir has 0.156 of average porosity and 493.7 md of average permeability. It contains light oil with an oil gravity of 33.4 °API and bubble point pressure of 1,205 psi. The drive mechanism of the reservoir is considered to be a strong water drive. The reservoir has formation water with 20,000 ppm salinity and ionic composition as shown in Table 1. The formation water composition indicates that there are divalent ions (Mg<sup>2+</sup> and Ca<sup>2+</sup>) in the reservoir that can contribute to ion exchange. The reservoir consists of 5 rock types. Three of them are mix wet and the rest are water wet. The reservoir also contains clay minerals including illite and kaolinite. These characteristics make the reservoir favorable for LSWI and LSWAG injection.

	Components	Concentration (ppm)
Cations	Na <sup>+</sup>	7,359.9
	Ca <sup>+</sup>	66.8
	Mg <sup>2+</sup>	13.8
	K <sup>+</sup>	74.7
	Ba <sup>2+</sup>	1.8
	Sr <sup>2+</sup>	18.7
Anions	Fe <sup>3+</sup>	3.2
	Cl <sup>-</sup>	9,059.4
	HCO <sub>3</sub> <sup>-</sup>	3,291.7
	SO <sub>4</sub> <sup>2-</sup>	120.9
<b>Total Salinity</b>		<b>20,010.9</b>

Table 1: Formation water composition of "B" Structure.

This study was completed by literature review and simulation study. The literature review was conducted to get a comprehensive understanding of the basic theories that are used in this study. The literature review covered the

## PROCEEDINGS

JOINT CONVENTION BANDUNG (JCB) 2021

November 23<sup>rd</sup> – 25<sup>th</sup> 2021

previous research and publications regarding LSWI, gas injection, water alternating gas (WAG), and LSWAG injection. The simulation study was started by learning the compositional simulator used in this study, namely CMG GEM<sup>TM</sup>. Afterward, data collection, fluid property modeling, and reservoir modeling were carried out. History matching was then also conducted to validate the reservoir model based on production history data. Finally, production forecasts and sensitivity studies were performed to achieve the objectives of this study.

Due to the unavailability of some experimental data, several assumptions were taken in the LSWAG modeling.

- Clay mineral content is distributed similarly to all grids.
- Interpolation range of equivalent fraction for ion exchange  $\zeta(\text{Na-X})$  is between 0.9378 and 0.6678 based on reservoir model initialization and default value in LSWI wizard menu of CMG GEM<sup>TM</sup>.

As one of the preliminary steps in reservoir simulation modeling, fluid property or PVT modeling was performed using CMG WINPROP<sup>TM</sup>. Based on the composition and the properties, the fluid of this reservoir can be categorized as light-medium oil. Fluid model matching to laboratory test results (Constant Composition Expansion and Differential Liberation) was also conducted to validate the model.

Minimum miscibility pressure (MMP) calculation was performed to determine whether the hydrocarbon injection is miscible or immiscible. Due to a lack of experimental data, the MMP was calculated using correlation. Ghorbani's correlation (2013) was chosen to calculate the MMP. Among all the MMP correlations commonly used for hydrocarbon gas, this correlation has criteria that best suit the characteristics of the reservoir fluid and the injection gas in this study. Additionally, unlike many other correlations, this correlation considers the composition of injection gas in its calculation. The calculation result gives 1,951 psi as the MMP value which is higher than the current and even initial reservoir pressure. It suggests that the gas flooding process in this case is immiscible. The MMP in the fluid model was then validated to the calculated MMP.

Reservoir initialization and history matching were performed to ensure that the reservoir model mimics the real condition and could give a valid forecast for this case study. The history matching was conducted by adjusting the aquifer parameters in the reservoir model. Production history data from 1998 until 2020 was used for the history matching process.

After the reservoir model had been validated by history matching, the production forecast for the base case was simulated to see the performance of the reservoir without LSWAG injection. The production forecast was simulated for 15 years, from 1<sup>st</sup> January 2021 until 1<sup>st</sup> January 2036, using B-1, B-3, and B-5 well as the production wells. The maximum production liquid rate of each well was limited to the liquid rate value at the end of history matching (546 BLPD for B-1, 2,342 BLPD for B-3, and 120 BLPD for B-5). The minimum bottom hole pressure (BHP) of each well was limited to 100 psi. An economic limit of 15 BOPD was also added to the production constraints of the forecast. The production forecast result is presented in Figure 3. From the oil rate profile of the forecast, compared to the other wells, B-1 produces the lowest oil rate and reaches the economic

limit too early in October 2027. Therefore, later in the LSWAG injection cases, B-1 was converted to an injection well in November 2027.

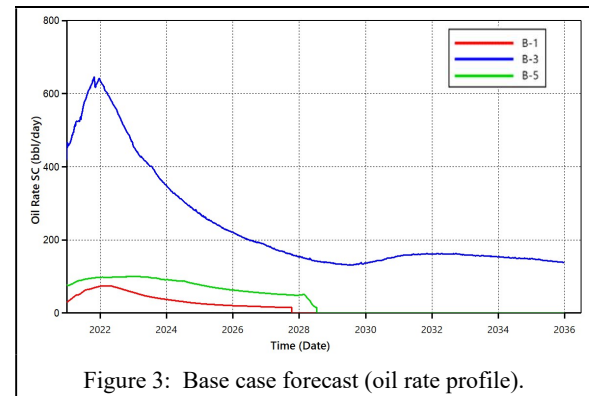


Figure 3: Base case forecast (oil rate profile).

Before proceeding to the other forecasts, LSWAG injection needs to be modeled first in the simulator. The LSWI part of the LSWAG injection was modeled through the LSWI wizard menu in CMG GEM<sup>TM</sup>. This simulator applies MIE as the main mechanism for LSWI. In the modeling process, formation water composition from ten ion analysis data was inputted into the simulator. A list of geochemical reactions which was obtained from analysis on PHREEQC Software was also entered into the simulator. As listed in Table 2, The geochemical reactions consist of aqueous reactions, mineral reactions, and cation exchange reactions. The cation exchange capacity (CEC) value for this reservoir was calculated using the equation from Seilsepour and Rashidi (2008), and the calculation result gave 237 eq/m<sup>3</sup> of CEC value. Wettability alteration through relative permeability shifting for this reservoir's rock types was modeled as well in the simulator. The interpolant ion used for this study was Na<sup>+</sup>. The shifting values can be seen in Table 3 which was obtained from laboratory experiment data that used 1,800 ppm of low salinity water. The initial point of ion exchange equivalent fraction  $\zeta(\text{Na-X})$  for interpolation was obtained from reservoir model initialization which gave the value of 0.9378. From the initial point and the default value of interpolation range in CMG GEM<sup>TM</sup>, the end point was assumed to be 0.6678. Figure 4 shows relative permeability shifting modeled in the simulator for one of the reservoir's rock types.

Reactions	
Aqueous Reaction	$\text{H}^+ + \text{OH}^- \leftrightarrow \text{H}_2\text{O}$
	$\text{CaHCO}_3^+ \leftrightarrow \text{Ca}^{2+} + \text{HCO}_3^-$
	$\text{NaHCO}_3 \leftrightarrow \text{Na}^+ + \text{HCO}_3^-$
	$\text{MgHCO}_3^+ \leftrightarrow \text{Mg}^{2+} + \text{HCO}_3^-$
	$\text{H}^+ + \text{NaCO}_3^- \leftrightarrow \text{Na}^+ + \text{HCO}_3^-$
Mineral Reaction	$\text{H}^+ + \text{Calcite} \leftrightarrow \text{Ca}^{2+} + \text{HCO}_3^-$
	$\text{H}^+ + \text{Dolomite} \leftrightarrow \text{Ca}^{2+} + \text{Mg}^{2+} + \text{HCO}_3^-$
Cation Exchange	$\text{Na}^+ + 0.5\text{Ca-X}_2 \leftrightarrow 0.5\text{Ca}^{2+} + \text{Na-X}$
	$\text{Na}^+ + 0.5\text{Mg-X}_2 \leftrightarrow 0.5\text{Mg}^{2+} + \text{Na-X}$

Table 2: Geochemical reactions.

Shifting Parameter	Value
K <sub>rw_LSWI</sub> /K <sub>rw_initial</sub>	0.247
K <sub>ro_LSWI</sub> /K <sub>ro_initial</sub>	1.098
Sor Reduction	0.039

Table 3: Relative permeability shifting value.

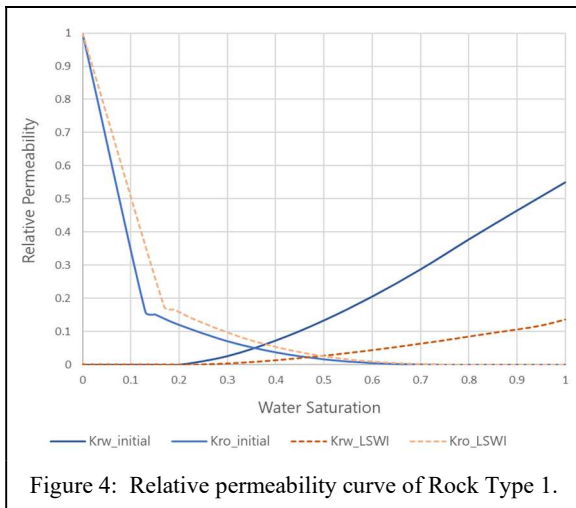


Figure 4: Relative permeability curve of Rock Type 1.

From the LSWI part, the modeling process was continued to the WAG part. The modeling was started by filling the injection gas composition. The injection gas composition was taken from the produced gas composition of the "S" field. The gas composition data are presented in Table 4. WAG ratio of 1:1 and WAG cycle of 1 cycle per year were used for this study. It means that 6 months of gas injection is followed by 6 months of low salinity water injection every year. These values were determined based on the previous study regarding CO<sub>2</sub>-LSWAG injection in the "T" Structure of the "S" Field which reported that 1:1 ratio and 1 cycle per year are the optimum values (Syah, 2020). Even though the structure and the injection gas type are different, it is assumed that they are also well applied in this study.

Component	Fraction
CO <sub>2</sub>	0.1243
N <sub>2</sub>	0.0086
CH <sub>4</sub>	0.3735
C <sub>2</sub> H <sub>6</sub>	0.0722
C <sub>3</sub> H <sub>8</sub>	0.2395
IC <sub>4</sub>	0.0504
NC <sub>4</sub>	0.0488
IC <sub>5</sub>	0.0352
NC <sub>5</sub>	0.0214
FC <sub>6</sub>	0.0113
C <sub>07+</sub>	0.0148

Table 4: Injection gas composition.

A sensitivity study was conducted by forecasting several LSWAG injection cases. These forecasts used the same production constraints (maximum liquid rate, minimum BHP, and economic limit) as those used in the base case forecast. The production wells used in this sensitivity study were also the same as the wells used in the base case (B-1, B-2, and B-3), but this time B-1 was converted to an injection well on 1<sup>st</sup> November 2027. Besides B-1, the suspended well, B-4, was also used as an injection well which started its LSWAG injection on 1<sup>st</sup> January 2022. Same as the base case, the LSWAG cases were also forecasted for 15 years. Three parameters were varied in this sensitivity study: injected water salinity, water injection rate, and gas injection rate.

- a. **Injected water salinity**  
 Injected water salinity is one of the main parameters which affect the performance of low salinity waterflooding. Since LSWAG involves low salinity waterflooding in its process, injected water salinity needs to be included in this sensitivity. There were two salinities used in this sensitivity: 1,800 ppm and 3,600 ppm. Their ionic composition can be seen in Table 5. The ionic strengths of these salinities are still higher than the Critical Total Ionic Strength (CTIS). Therefore, there is no formation damage, and these salinities are safe to use.
- b. **Water injection rate**  
 Besides salinity, water injection rate also affects the performance of the low salinity waterflooding in LSWAG. The water injection rate in this sensitivity was limited to a maximum of 1,500 BHPD per injection well. This is due to the availability of produced water in "B" structure that can only supply around that quantity. The water injection rate in this sensitivity was then varied to 500 BHPD, 1,000 BHPD, and 1,500 BHPD per well.
- c. **Gas injection rate**  
 Gas injection rate affects the gas flooding performance in LSWAG. Like the water injection rate, the gas injection rate in this sensitivity was also limited due to the availability of produced gas in the "S" field. The gas injection rate was limited to a maximum of 1 MMSCFD per injection well. Therefore, the gas injection rate in this study was varied to 0.25 MMSCFD, 0.5 MMSCFD, and 1 MMSCFD per well.

Components	Concentration (ppm)		
	A	B	
Cations	Na <sup>+</sup>	662.10	1,324.20
	Ca <sup>+</sup>	6.01	12.02
	Mg <sup>2+</sup>	1.24	2.48
	K <sup>+</sup>	6.72	13.44
	Ba <sup>2+</sup>	0.16	0.32
	Sr <sup>2+</sup>	1.68	3.36
	Fe <sup>3+</sup>	0.29	0.58
Anions	Cl <sup>-</sup>	814.98	1,629.96
	HCO <sub>3</sub> <sup>-</sup>	296.12	592.25
	SO <sub>4</sub> <sup>2-</sup>	10.88	21.75
<b>Total Salinity</b>	<b>1,800</b>	<b>3,600</b>	

Table 5: Injection water ionic composition.

All permutation cases from the three parameters above were forecasted. In total there were 18 cases forecasted. From those forecasts, the impact of each parameter variation on the recovery factor could be analyzed. The optimum combination which gives the highest recovery factor could also be determined.

**Result and Discussion**

Simulation result of the LSWAG injection cases is presented in Table 6. From the table, all the 1,800 ppm cases give a higher recovery factor than the 3,600 ppm cases. These results align with the LSWI theory which stated that lower salinity results in more shifting towards water wet and thus more oil recovery. That is because lower salinity promotes

**PROCEEDINGS**

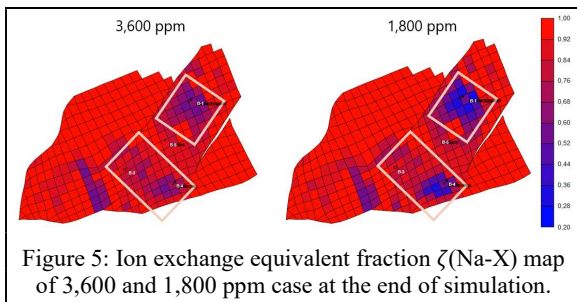
**JOINT CONVENTION BANDUNG (JCB) 2021**

November 23<sup>rd</sup> – 25<sup>th</sup> 2021

more ion exchanges in the flooding process. Since the simulator used in this study takes MIE as the underlying mechanism of LSWI, the distribution of ion exchange equivalent fraction in the reservoir at the end of forecast can be displayed in a map. Figure 5 presents one pair example of 1,800 ppm and 3,600 ppm cases which have the same values on other parameters (Both used 1,500 BWPD of water injection rate and 0.5 MMSCFD of gas injection rate). Compared to the 3,600 ppm case, the 1,800 ppm case results in a lower ion exchange equivalent fraction  $\zeta(\text{Na-X})$  which means more ion exchanges have occurred.

Water Inj. Rate (BWPD)	Gas Inj. Rate (MMSCFD)	Recovery Factor (%)	
		1800 ppm	3600 ppm
500	0.25	58.05	58.01
	0.5	58.61	58.59
	1	60.10	60.07
1000	0.25	59.44	59.34
	0.5	60.02	59.92
	1	61.38	61.30
1500	0.25	60.31	60.21
	0.5	61.09	60.84
	1	62.34	62.24

Table 6: Simulation results of LSWAG injection cases.



From the sensitivity study result in Table 6, it can be concluded also that recovery factor is directly proportional to water injection rate, meaning the higher the water injection rate, the higher the recovery factor will be. This correlation applies to all gas injection rates and all water salinity. A higher water injection rate means a higher volume of water being injected into the reservoir and more area in the reservoir being swept by the injected water. This improves the macroscopic sweep efficiency of the flooding process. The cation exchange and wettability alteration also take place in a wider area in the reservoir. Figure 6 displays the distribution of ion exchange equivalent fraction at the end of simulation for a pair of simulation cases with the same salinity and gas injection rate but different water injection rate. Compared to the 500 BWPD case, the 1,500 BWPD case shows a wider area impacted by ion exchange and wettability alteration. This result is also confirmed by the oil saturation distribution across the reservoir at the end of simulation. Figure 7 shows the remaining oil saturation across reservoir from B-3 to B-4 at the end of simulation. B-3 is chosen because the incremental of oil recovery mostly comes from B-3. The 1,500 BWPD case gives lower remaining oil saturation than the 500 BWPD case. For water injection rates higher than 1,500 BWPD, it might still give a

higher recovery factor. However, as mentioned in the previous section, this sensitivity is limited to a maximum of 1,500 BWPD due to the availability of produced water in the "B" Structure.

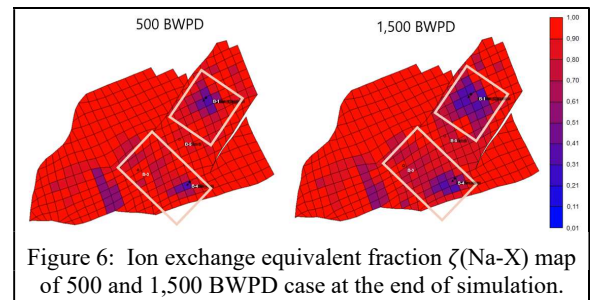


Figure 6: Ion exchange equivalent fraction  $\zeta(\text{Na-X})$  map of 500 and 1,500 BWPD case at the end of simulation.

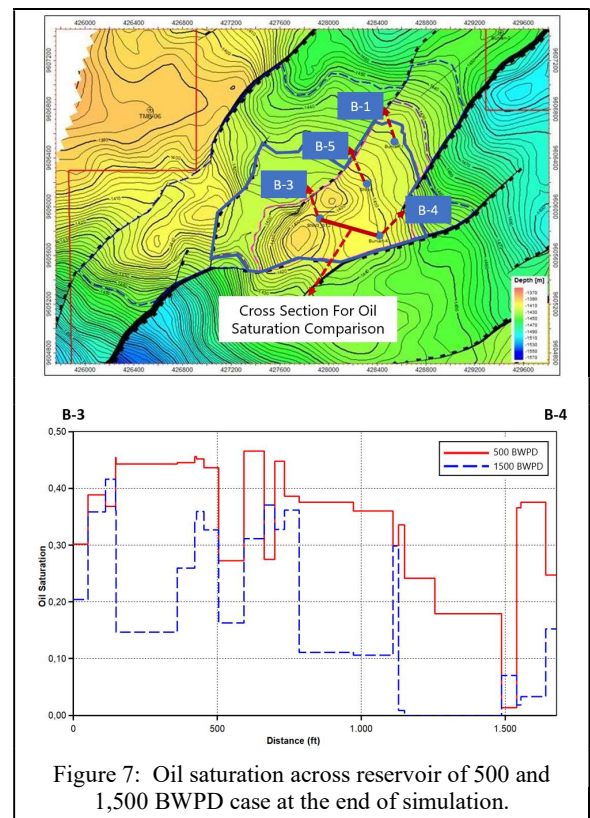


Figure 7: Oil saturation across reservoir of 500 and 1,500 BWPD case at the end of simulation.

Besides water injection rate impact, gas injection rate impact can be inferred as well from the simulation result in Table 6. It shows that recovery factor increases as gas injection rate increases. This linearity applies to all water injection rates and salinity. This is because a higher gas injection rate promotes more viscosity reduction and oil swelling to occur in the reservoir. The mechanisms are viscosity reduction and oil swelling because the reservoir pressure during gas injection has confirmed that the gas flooding process was immiscible. Figure 8 displays viscosity distribution map at the end of simulation for two cases with different gas injection rate but the same injected water salinity and water injection rate (1,800 ppm and 500 BWPD). The figure indicates that higher gas injection rate causes higher viscosity reduction. The viscosity reduction in combination with oil swelling reduces mobility ratio and thus improves sweep efficiency. This result is also proved by the oil saturation distribution across reservoir at the end of simulation. Figure 9 shows that the remaining oil saturation

across reservoir from B-3 to B-4 at the end of simulation in 1 MMSCFD case is lower than that in 0.25 MMSCFD case. Like the water injection rate sensitivity, gas injection rates higher than 1 MMSCFD may give a higher recovery factor, but it is not simulated due to the limitation of produced gas availability in the "S" Field.

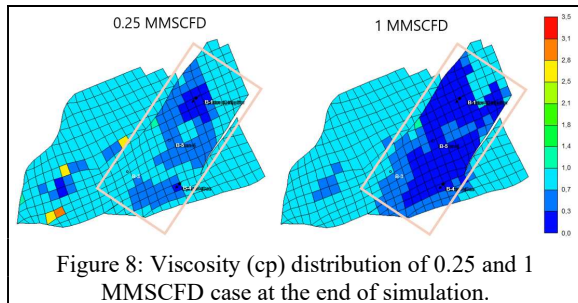
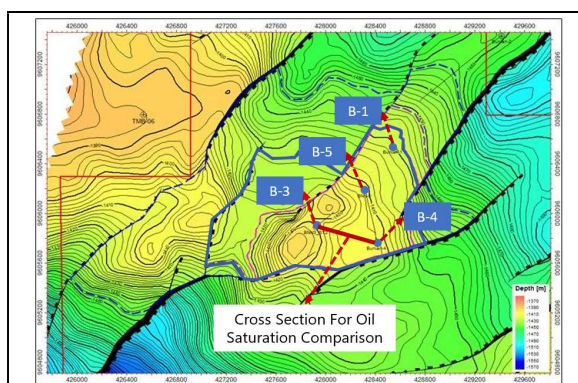


Figure 8: Viscosity (cp) distribution of 0.25 and 1 MMSCFD case at the end of simulation.



Cross Section For Oil Saturation Comparison

Figure 9: Oil saturation across reservoir of 0.25 and 1 MMSCFD case at the end of simulation.

Finally, based on the simulation result, the optimum design which gives the highest recovery factor is the case that uses 1,800 ppm of injected water salinity, 1,500 BWPD of water injection rate, and 1 MMSCFD of gas injection rate. This optimum design can give 62.34% of recovery factor which means a 7.81% increase from base case. The increase equals 0.56 MMSTB of oil cumulative production. It should be noted that the optimum design is obtained after considering the limitation in the fields such as the availability of produced gas and water. Based on the result, it is known that LSWAG injection is a very promising method to be implemented in terms of oil recovery. Not to mention the utilization of hydrocarbon gas as the injection gas in this method is very good for environment since it reduces flaring activity.

## Conclusions

Based on the analysis and discussion above, the following conclusions regarding LSWAG injection implementation at "B" Structure in "S" Field can be taken.

- Oil recovery is inversely proportional to injected water salinity. It increases as the injected water salinity decreases due to more shifting toward water wet. On the other hand, oil recovery is directly proportional to water injection rate and gas injection rate. The higher the water and gas injection rate, the higher the recovery factor is. It happens because higher injection rates promote mobility ratio reduction and sweep efficiency improvement. This correlation applies until the maximum value of water and gas injection rate which are available in the field.
- The optimum design for LSWAG implementation at "B" Structure in "S" Field is by using 1,800 ppm of injected water salinity, 1,500 BWPD of water injection rate, and 1 MMSCFD of gas injection rate. This optimum condition considers the availability of water and gas for injection in the field.

To further improve the results of this study, another sensitivity study on operational parameters such as WAG ratio and WAG cycle can be performed. Additionally, production and injection scenario sensitivity such as infill drilling can also be conducted to assess the possibility of better LSWAG performance.

## References

- Christensen, J. R., Stenby, E. H., & Skauge, A., 2001, SPE Reservoir Evaluation & Engineering, **4**, 97-106.
- Dang, T. Q. C., Nghiem, L., Nguyen, N., Chen, Z., and Nguyen, Q. P., 2014, SPE Improved Oil Recovery Symposium, Tulsa, Oklahoma, USA, 12-16 April.
- Dang, T. Q. C., Nghiem, L., Nguyen, N., Chen, Z., and Nguyen, Q. P., 2015, SPE Western Regional Meeting, Garden Grove, California, USA, 27-30 April.
- Dong, J., Wu, S., Xing, G., Fan, T., Li, H., & Wang, B., 2019, International Petroleum Technology Conference, Beijing, China, 26-28 March.
- Ghorbani, M., Momeni, A., & Morady, B., 2013, Petroleum Science and Technology, **31**, 2577-2584.
- Holtz, M. H., 2016, SPE Improved Oil Recovery Conference, Tulsa, Oklahoma, USA, 11-13 April.
- Lager, A., Webb, K. J., Black, C. J. J., Singleton, M., & Sorbie, K. S., 2008, Petrophysics - The SPWLA Journal of Formation Evaluation and Reservoir Description, **49**, 28-35.
- Ning, X. S. & McGuire, P. L., 2004, SPE/DOE Fourteenth Symposium on Improved Oil Recovery, Tulsa, Oklahoma, USA, 17-21 April.
- Permadi, A. K., 2019, Scientific Speech, Institut Teknologi Bandung, 23 November.
- Seilsepour, M. & Rashidi, M., 2008, World Applied Sciences Journal, **3**, 200-205.
- Syah, G. A. A., 2020, B.S.E. thesis, Institut Teknologi Bandung.

## Acknowledgments

The authors would like to extend their highest gratitude to Bass Oil Sukananti Limited for providing full support including guidance and field data for this study.